Searches for sleptons and squarks in e^+e^- collisions at 189 GeV

R. Barate, D. Decamp, P. Ghez, C. Goy, S. Jezequel, J.P. Lees, F. Martin, E. Merle, M.N. Minard, B. Pietrzyk, et al.

EUROPEAN LABORATORY FOR PARTICLE PHYSICS (CERN)

CERN-EP 99-140
7 October 1999

Searches for sleptons and squarks in e^+e^- collisions at 189 GeV

The ALEPH Collaboration

Abstract

The data collected at a centre-of-mass energy of 188.6 GeV by ALEPH at LEP, corresponding to an integrated luminosity of 173.6 pb^{-1}, are analysed in a search for the scalar partners of quarks and leptons predicted in supersymmetric models. No evidence for any such particles was found in the decay channels $\tilde{\ell} \to \ell\chi$, $\tilde{t} \to c\chi$, $\tilde{t} \to b\ell\tilde{\nu}$, $\tilde{b} \to b\chi$, and $\tilde{q} \to q\chi$. Improved mass lower limits have been obtained in the framework of the Minimal Supersymmetric Standard Model.

(To be submitted to Physics Letters B)

The ALEPH Collaboration

R. Barate, D. Decamp, P. Ghez, C. Goy, S. Jezequel, J.-P. Lees, F. Martin, E. Merle, M.-N. Minard, B. Pietrzyk

Laboratoire de Physique des Particules (LAPP), IN^{2}P^3-CNRS, F-74019 Annecy-le-Vieux Cedex, France

R. Alemany, S. Bravo, M.P. Casado, M. Chmeissani, J.M. Crespo, E. Fernandez, M. Fernandez-Bosman, Ll. Garrido,[15] E. Graugès, A. Juste, M. Martinez, G. Merino, R. Miquel, Ll.M. Mir, P. Morawitz, A. Pacheco, I. Riu, H. Ruiz

Institut de Física d'Altes Energies, Universitat Autònoma de Barcelona, 08193 Bellaterra (Barcelona), E-Spain[7]

A. Colaleo, D. Creanza, M. de Palma, G. Iaselli, G. Maggi, M. Maggi, S. Nuzzo, A. Ranieri, G. Raso, F. Ruggieri, G. Selvaggi, L. Silvestris, P. Tempesta, A. Tricomi,[3] G. Zito

Dipartimento di Fisica, INFN Sezione di Bari, I-70126 Bari, Italy

X. Huang, J. Lin, Q. Ouyang, T. Wang, Y. Xie, R. Xu, S. Xue, J. Zhang, L. Zhang, W. Zhao

Institute of High-Energy Physics, Academia Sinica, Beijing, The People's Republic of China[8]

D. Abbaneo, G. Boix,[6] O. Buchmüller, M. Cattaneo, F. Cerutti, V. Ciulli, G. Davies, G. Dissertori, H. Drevermann, R.W. Forty, M. Frank, F. Gianotti, T.C. Greening, A.W. Halley, J.B. Hansen, J. Harvey, P. Janot, B. Jost, M. Kado, O. Leroy, P. Maley, P. Mato, A. Minten, A. Moutoussi, F. Ranjard, L. Rolandi, D. Schlatter, M. Schmitt,[20] O. Schneider,[2] P. Spagnolo, W. Tejessy, F. Teubert, E. Tournefier, A.E. Wright

European Laboratory for Particle Physics (CERN), CH-1211 Geneva 23, Switzerland

Z. Ajaltouni, F. Badaud G. Chazelle, O. Deschamps, S. Dessagne, A. Falvard, C. Ferdi, P. Gay, C. Guicheney, P. Henrard, J. Jousset, B. Michel, S. Monteil, J-C. Montret, D. Pallin, J.M. Pascolo, P. Perret, F. Podlyski

Laboratoire de Physique Corpusculaire, Université Blaise Pascal, IN^{2}P^3-CNRS, Clermont-Ferrand, F-63177 Aubière, France

J.D. Hansen, J.R. Hansen, P.H. Hansen,1 B.S. Nilsson, B. Rensch, A. Wäänänen

Niels Bohr Institute, 2100 Copenhagen, DK-Denmark[9]

G. Daskalakis, A. Kyriakis, C. Markou, E. Simopoulou, A. Vayaki

Nuclear Research Center Demokritos (NRCD), GR-15310 Attiki, Greece

A. Blondel, J.-C. Brient, F. Machefert, A. Rougé, M. Swynghedauw, R. Tanaka, A. Valassi,[23] H. Videau

Laboratoire de Physique Nucléaire et des Hautes Energies, Ecole Polytechnique, IN^{2}P^3-CNRS, F-91128 Palaiseau Cedex, France

E. Focardi, G. Parrini, K. Zachariadou

Dipartimento di Fisica, Università di Firenze, INFN Sezione di Firenze, I-50125 Firenze, Italy

M. Corden, C. Georgiopoulos

Supercomputer Computations Research Institute, Florida State University, Tallahassee, FL 32306-4052, USA [13,14]

A. Antonelli, G. Bencivenni, G. Bologna,[4] F. Bossi, P. Campana, G. Capon, V. Chiarella, P. Laurelli, G. Mannocchi,[1,5] F. Murtas, G.P. Murtas, L. Passalacqua, M. Pepe-Altarelli

Laboratori Nazionali dell'INFN (LNF-INFN), I-00044 Frascati, Italy

M. Chalmers, L. Curtis, J.G. Lynch, P. Negus, V. O'Shea, B. Raeven, C. Raine, D. Smith, P. Teixeira-Dias, A.S. Thompson, J.J. Ward

Department of Physics and Astronomy, University of Glasgow, Glasgow G12 8QQ,United Kingdom[10]

R. Cavanaugh, S. Dhamotharan, C. Geweniger,[1] P. Hanke, V. Hepp, E.E. Kluge, A. Putzer, K. Tittel, S. Werner,[19] M. Wunsch[19]

Institut für Hochenergiephysik, Universität Heidelberg, D-69120 Heidelberg, Germany[16]

R. Beuselinck, D.M. Binnie, W. Cameron, P.J. Dornan, M. Girone, S. Goodsir, N. Marinelli, E.B. Martin, J. Nash, J. Nowell, H. Przysiezniak,[1] A. Sciabà, J.K. Sedgbeer, E. Thomson, M.D. Williams

Department of Physics, Imperial College, London SW7 2BZ, United Kingdom[10]

V.M. Ghete, P. Girtler, E. Kneringer, D. Kuhn, G. Rudolph

Institut für Experimentalphysik, Universität Innsbruck, A-6020 Innsbruck, Austria[18]

C.K. Bowdery, P.G. Buck, G. Ellis, A.J. Finch, F. Foster, G. Hughes, R.W.L. Jones, N.A. Robertson, M. Smizanska, M.I. Williams

Department of Physics, University of Lancaster, Lancaster LA1 4YB, United Kingdom[10]

I. Giehl, F. Hölldorfer, K. Jakobs, K. Kleinknecht, M. Kröcker, A.-S. Müller, H.-A. Nürnberger, G. Quast, B. Renk, E. Rohne, H.-G. Sander, S. Schmeling, H. Wachsmuth C. Zeitnitz, T. Ziegler

Institut für Physik, Universität Mainz, D-55099 Mainz, Germany[16]

J.J. Aubert, A. Bonissent, J. Carr, P. Coyle, A. Ealet, D. Fouchez, A. Tilquin

Centre de Physique des Particules, Faculté des Sciences de Luminy, IN^{2}P^3-CNRS, F-13288 Marseille, France

M. Aleppo, M. Antonelli, S. Gilardoni, F. Ragusa

Dipartimento di Fisica, Università di Milano e INFN Sezione di Milano, I-20133 Milano, Italy.

V. Büscher, H. Dietl, G. Ganis, K. Hüttmann, G. Lütjens, C. Mannert, W. Männer, H.-G. Moser, S. Schael, R. Settles, H. Seywerd, H. Stenzel, W. Wiedenmann, G. Wolf

Max-Planck-Institut für Physik, Werner-Heisenberg-Institut, D-80805 München, Germany[16]

P. Azzurri, J. Boucrot, O. Callot, S. Chen, M. Davier, L. Duflot, J.-F. Grivaz, Ph. Heusse, A. Jacholkowska,[1] J. Lefrançois, L. Serin, J.-J. Veillet, I. Videau,[1] J.-B. de Vivie de Régie, D. Zerwas

Laboratoire de l'Accélérateur Linéaire, Université de Paris-Sud, IN^{2}P^3-CNRS, F-91898 Orsay Cedex, France

G. Bagliesi, T. Boccali, C. Bozzi,[12] G. Calderini, R. Dell'Orso, I. Ferrante, A. Giassi, A. Gregorio, F. Ligabue, P.S. Marrocchesi, A. Messineo, F. Palla, G. Rizzo, G. Sanguinetti, G. Sguazzoni, R. Tenchini,[1] A. Venturi, P.G. Verdini

Dipartimento di Fisica dell'Università, INFN Sezione di Pisa, e Scuola Normale Superiore, I-56010 Pisa, Italy

G.A. Blair, J. Coles, G. Cowan, M.G. Green, D.E. Hutchcroft, L.T. Jones, T. Medcalf, J.A. Strong

Department of Physics, Royal Holloway & Bedford New College, University of London, Surrey TW20 OEX, United Kingdom[10]

D.R. Botterill, R.W. Clifft, T.R. Edgecock, P.R. Norton, J.C. Thompson, I.R. Tomalin

Particle Physics Dept., Rutherford Appleton Laboratory, Chilton, Didcot, Oxon OX11 OQX, United Kingdom[10]

B. Bloch-Devaux, P. Colas, B. Fabbro, G. Faïf, E. Lançon, M.-C. Lemaire, E. Locci, P. Perez, J. Rander, J.-F. Renardy, A. Rosowsky, P. Seager,[24] A. Trabelsi,[21] B. Tuchming, B. Vallage

CEA, DAPNIA/Service de Physique des Particules, CE-Saclay, F-91191 Gif-sur-Yvette Cedex, France[17]

S.N. Black, J.H. Dann, C. Loomis, H.Y. Kim, N. Konstantinidis, A.M. Litke, M.A. McNeil, G. Taylor

Institute for Particle Physics, University of California at Santa Cruz, Santa Cruz, CA 95064, USA[22]

C.N. Booth, S. Cartwright, F. Combley, P.N. Hodgson, M. Lehto, L.F. Thompson

Department of Physics, University of Sheffield, Sheffield S3 7RH, United Kingdom[10]

K. Affholderbach, A. Böhrer, S. Brandt, C. Grupen, J. Hess, A. Misiejuk, G. Prange, U. Sieler

Fachbereich Physik, Universität Siegen, D-57068 Siegen, Germany[16]

C. Borean, G. Giannini, B. Gobbo

Dipartimento di Fisica, Università di Trieste e INFN Sezione di Trieste, I-34127 Trieste, Italy

J. Putz, J. Rothberg, S. Wasserbaech, R.W. Williams

Experimental Elementary Particle Physics, University of Washington, WA 98195 Seattle, U.S.A.

S.R. Armstrong, P. Elmer, D.P.S. Ferguson, Y. Gao, S. González, O.J. Hayes, H. Hu, S. Jin, J. Kile, P.A. McNamara III, J. Nielsen, W. Orejudos, Y.B. Pan, Y. Saadi, I.J. Scott, J. Walsh, J.H. von Wimmersperg-Toeller, Sau Lan Wu, X. Wu, G. Zobernig

Department of Physics, University of Wisconsin, Madison, WI 53706, USA[11]

[1]Also at CERN, 1211 Geneva 23, Switzerland.

[2]Now at Université de Lausanne, 1015 Lausanne, Switzerland.

[3]Also at Centro Siciliano di Fisica Nucleare e Struttura della Materia, INFN Sezione di Catania, 95129 Catania, Italy.

[4]Also Istituto di Fisica Generale, Università di Torino, 10125 Torino, Italy.

[5]Also Istituto di Cosmo-Geofisica del C.N.R., Torino, Italy.

[6]Supported by the Commission of the European Communities, contract ERBFMBICT982894.

[7]Supported by CICYT, Spain.

[8]Supported by the National Science Foundation of China.

[9]Supported by the Danish Natural Science Research Council.

[10]Supported by the UK Particle Physics and Astronomy Research Council.

[11]Supported by the US Department of Energy, grant DE-FG0295-ER40896.

[12]Now at INFN Sezione di Ferrara, 44100 Ferrara, Italy.

[13]Supported by the US Department of Energy, contract DE-FG05-92ER40742.

[14]Supported by the US Department of Energy, contract DE-FC05-85ER250000.

[15]Permanent address: Universitat de Barcelona, 08208 Barcelona, Spain.

[16]Supported by the Bundesministerium für Bildung, Wissenschaft, Forschung und Technologie, Germany.

[17]Supported by the Direction des Sciences de la Matière, C.E.A.

[18]Supported by the Austrian Ministry for Science and Transport.

[19]Now at SAP AG, 69185 Walldorf, Germany

[20]Now at Harvard University, Cambridge, MA 02138, U.S.A.

[21]Now at Département de Physique, Faculté des Sciences de Tunis, 1060 Le Belvédère, Tunisia.

[22]Supported by the US Department of Energy, grant DE-FG03-92ER40689.

[23]Now at LAL, 91898 Orsay, France.

[24]Supported by the Commission of the European Communities, contract ERBFMBICT982874.

1 Introduction

In the Minimal Supersymmetric extension of the Standard Model (MSSM) [1], each Standard Model fermion chirality state has a scalar supersymmetric partner. The sfermions $\tilde{\mathrm{f}}_{\mathrm{R}}$ and $\tilde{\mathrm{f}}_{\mathrm{L}}$ are the supersymmetric partners of the right-handed and left-handed fermions, respectively. These are weak eigenstates which can mix to form the mass eigenstates. The mixing is a unitary transformation of the $\tilde{\mathrm{f}}_{\mathrm{R}}$ and $\tilde{\mathrm{f}}_{\mathrm{L}}$ states, parameterised by a mixing angle θ. Because the off-diagonal elements of the sfermion mass matrix are proportional to the SM partner masses, the mixing is expected to be relevant for the scalar top (stop, $\tilde{\mathrm{t}}$), scalar bottom (sbottom, $\tilde{\mathrm{b}}$) and scalar tau (stau, $\tilde{\tau}$).

Sfermions can be produced at LEP in pairs, $\mathrm{e^+e^-} \to \tilde{\mathrm{f}}\bar{\tilde{\mathrm{f}}}$, via s-channel exchange of a virtual photon or a Z, whereas the t-channel exchange of neutralinos can contribute in the case of selectron ($\tilde{\mathrm{e}}$) production, making possible, for this flavour, the mixed production $\tilde{\mathrm{e}}_{\mathrm{R}}\tilde{\mathrm{e}}_{\mathrm{L}}$ when kinematically allowed.

The searches for sfermions described here assume that the lightest supersymmetric particle (LSP) is the lightest neutralino χ or possibly the sneutrino. The conservation of R-parity is also assumed; this implies that supersymmetric particles are produced in pairs and that the LSP is stable.

Under these assumptions, all the sfermions but the stop decay predominantly as $\tilde{\mathrm{f}} \to \mathrm{f}\chi$ (the decay $\tilde{\mathrm{t}} \to \mathrm{t}\chi$ is kinematically inaccessible at LEP2). The stop can decay as $\tilde{\mathrm{t}} \to \mathrm{c}\chi$ or $\tilde{\mathrm{t}} \to \mathrm{b}\ell\tilde{\nu}$ [2]. The first decay can proceed only via loop diagrams and thus has a very small width, of the order of 0.01–1 eV [2]. The $\tilde{\mathrm{t}} \to \mathrm{b}\ell\tilde{\nu}$ channel proceeds via virtual chargino exchange and has a width of the order of 0.1–10 keV [2]. The latter decay dominates when it is kinematically allowed.

Direct searches for squarks and sleptons were performed in the dominant decay channels mentioned above. The final states studied are summarized in Table 1. As described in Ref.[4], the search for mixed selectron production extends the sensitivity of the selectron searches to situations where the acoplanar electron search is ineffective because of the small mass difference between the lightest selectron and the lightest neutralino. In this case the outgoing lepton from the decay of the heaviest selectron (typically the $\tilde{\mathrm{e}}_{\mathrm{L}}$) has enough energy to be detected, leading to a single electron topology.

Table 1: Topologies studied in the different scenarios.

Production	Decay mode	Topology
$\tilde{\mathrm{q}}\bar{\tilde{\mathrm{q}}}$	$\tilde{\mathrm{q}} \to \mathrm{q}\chi$	Acoplanar jets
$\tilde{\mathrm{t}}\bar{\tilde{\mathrm{t}}}$	$\tilde{\mathrm{t}} \to \mathrm{c}\chi$	Acoplanar jets
$\tilde{\mathrm{b}}\bar{\tilde{\mathrm{b}}}$	$\tilde{\mathrm{b}} \to \mathrm{b}\chi$	Acoplanar b-jets
$\tilde{\mathrm{t}}\bar{\tilde{\mathrm{t}}}$	$\tilde{\mathrm{t}} \to \mathrm{b}\ell\tilde{\nu}$	Acoplanar jets plus leptons
$\tilde{\ell}\bar{\tilde{\ell}}$	$\tilde{\ell} \to \ell\chi$	Acoplanar leptons
$\tilde{\mathrm{e}}_{\mathrm{L,(R)}}\bar{\tilde{\mathrm{e}}}_{\mathrm{R,(L)}}$	$\tilde{\mathrm{e}} \to \mathrm{e}\chi$	Single electron (small $m_{\tilde{\mathrm{e}}_{\mathrm{R}}} - m_{\chi}$)

Data collected at $\sqrt{s}$ = 188.6 GeV and corresponding to an integrated luminosity of 173.6 pb^{-1} have been analysed. The results of these searches supersede the ALEPH results reported earlier for data collected at energies up to $\sqrt{s}$ = 184 GeV [3, 4]. Searches for light stop and sbottom have also been performed at the Tevatron [5, 6]. The CDF experiment [6] has reported a lower limit on the stop mass of about 120 GeV/c^2 for the decay into cχ and a lower limit on the sbottom mass of about 140 GeV/c^2 for the decay into bχ; these limits are valid for a mass difference between the $\tilde{\mathrm{q}}$ and the χ larger than about 40 GeV/c^2. The D0 and CDF Collaborations have also published limits on squark masses under the assumption that u, d, s, c and b squarks are mass degenerate [7].

Searches for squarks and sleptons using data collected at LEP at energies up to $\sqrt{s}$ = 189 GeV have also been performed by OPAL [8].

2 The ALEPH detector

A detailed description of the ALEPH detector can be found in Ref. [9], and an account of its performance as well as a description of the standard analysis algorithms can be found in Ref. [10]. Only a brief overview is given here.

Charged particles are detected in a magnetic spectrometer consisting of a silicon vertex detector (VDET), a drift chamber (ITC) and a time projection chamber (TPC), all immersed in a 1.5 T axial magnetic field provided by a superconducting solenoid. The VDET consists of two cylindrical layers of silicon microstrip detectors; it performs precise measurements of the impact parameter in space thus allowing powerful short-lifetime particle tags, as described in Ref. [11]. Between the TPC and the coil, a highly granular electromagnetic calorimeter (ECAL) is used to identify electrons and photons and to measure their energies. Surrounding the ECAL is the return yoke for the magnet, which is instrumented with streamer tubes to form the hadron calorimeter (HCAL). Two layers of external streamer tubes are used together with the HCAL to identify muons. The region near the beam line is covered by two luminosity calorimeters, SICAL and LCAL, which provide coverage down to 34 mrad. The information obtained from the tracking system is combined with that from the calorimeters to form a list of "energy flow particles" [10]. These objects are used to calculate the variables that are employed in the analyses described in Section 3.

3 The selections

Several selection algorithms have been developed to search for squarks and sleptons. Events with acoplanar jets and acoplanar jets plus two leptons are signatures for squark production. Events with acoplanar lepton pairs or with single electrons are expected from slepton production. All these channels are characterised by missing energy.

The event properties depend significantly on Δm, the mass difference between the decaying sfermion and the produced χ or $\tilde{\nu}$. When Δm is large, there is a substantial amount of energy available for the visible system and the signal events tend to look like WW, Weν, Zγ^*, and q$\bar{\mathrm{q}}(\gamma)$ events. When Δm is small, the energy available for the visible system is small and

the signal events are therefore similar to $\gamma\gamma$ events. In order to cope with the different signal topologies and background situations, each analysis employs a low Δm selection and a high Δm selection. The optimization of the selection criteria, as well as the best combination of the high and low Δm analyses, have been obtained by minimization of the expected 95 % C.L. cross section upper limit in the absence of signal (the $\bar{N}_{95}$ prescription [12]). The selections applied to the 189 GeV data follow closely those described in Refs. [3, 4]. The selection cuts have been re-optimized to take into account the increased centre-of-mass energy and the larger integrated luminosity. Additional cuts have also been introduced for the acoplanar jets (low Δm selection) and for the stau selections.

3.1 Acoplanar jet selection

The acoplanar jet selection is used to search for the processes $e^+e^- \to \tilde{q}\bar{\tilde{q}}$ ($\tilde{q} \to q\chi$). The same cuts used in Ref. [3] to reject the $\gamma\gamma \to q\bar{q}$ background are applied after an appropriate rescaling with the centre-of-mass energy. For the low Δm selection a new cut has been included: the number of charged tracks in a jet is required to be greater than one. This cut reduces the background contamination from WW and $\gamma\gamma$ processes producing $\tau \to$ one-prong final states.

For large Δm, a few changes have been made in order to cope with the increased level of background from WW, Weν, and Zγ^* that results from the increased integrated luminosity. The $M_{\rm vis}/\sqrt{s}$ cut has been tightened. The position of the cut depends on the Δm of the signal being considered. For $\Delta m = 15$ GeV/c^2 the optimal cut is $M_{\rm vis}/\sqrt{s} < 0.20$, while for $\Delta m = 25$ GeV/c^2 the optimal cut is $M_{\rm vis}/\sqrt{s} < 0.25$. Finally, the optimal cut for all Δm greater than 40 GeV/c^2 is $M_{\rm vis}/\sqrt{s} < 0.30$.

The low Δm selection is used for $\Delta m < 8$ GeV/c^2, while for $\Delta m \geq 8$ GeV/c^2 the high Δm selection is used. The background to the low Δm selection is dominated by $\gamma\gamma \to q\bar{q}$ and has a total expectation of 5.5 events (~ 32 fb). For the high Δm selection, the background is dominated by WW, Weν, Zγ^*, and $q\bar{q}(\gamma)$. If the loosest value of the upper cut on $M_{\rm vis}$ is applied, the total background expectation for the high Δm selection is 4.0 events (~ 23 fb).

The experimental topology of the $e^+e^- \to \tilde{b}\bar{\tilde{b}}$ ($\tilde{b} \to b\chi$) process is characterised by two acoplanar b jets and missing mass and energy. The selection used to search for this topology is quite similar to that used at lower energies [3]; here only the differences are described.

For the high Δm selection, the WW, Zγ^* and Weν backgrounds are reduced by taking advantage of the presence of b jets. The events are tagged by using the b tag event probability $P_{\rm uds}$ described in [11]. The two-dimensional cut in the ($M_{\rm vis}$,$P_{\rm uds}$) plane described in [3] has been tightened to cope with the increased background.

The optimization chooses the low Δm selection for $\Delta m < 12$ GeV/c^2 and the high Δm selection for $\Delta m > 12$ GeV/c^2. The total background expectation for the low Δm selection is 3.3 events (19 fb), dominated by $\gamma\gamma \to q\bar{q}$. For the high Δm selection the WW, Zγ^*, and Weν background is highly suppressed by b tagging and the total background expectation is 0.9 events (5 fb).

3.2 Acoplanar jet plus leptons selection

The experimental signature for $e^+e^- \to \tilde{t}\bar{\tilde{t}}$ ($\tilde{t} \to b\ell\tilde{\nu}$) production is two acoplanar jets plus two leptons with missing momentum. For this search the same selection as in [3] is applied.

For $\Delta m < 11$ GeV/c^2, the logical OR of the high and low Δm selections is used: the high Δm selection helps to increase the efficiency while leaving the background level unchanged. For $\Delta m \geq 11$ GeV/c^2, only the high Δm selection is used. The background to the low Δm selection is dominated by $\gamma\gamma \to q\bar{q}$ and has a total expectation of 1.9 events (11 fb). For the high Δm selection, the 2.5 fb of expected background (0.4 events expected) is dominated by WW and $q\bar{q}$ events.

3.3 Acoplanar lepton selection

Slepton pair production leads to a final state characterized by two acoplanar leptons of the same flavour and missing mass and energy; acoplanar lepton selections are used to search for these processes. The selections developed for the 183 GeV data [4] are optimized to account for the increase in energy and luminosity, as well as the changes in the composition of the background. The background from the leptonic WW processes is subtracted in the optimization. In the following a detailed description of the new or modified cuts is given.

In the search for selectrons and smuons with high Δm the same selections as in [4] are applied. In the low Δm selection the cut based on the Fisher discriminant analysis has been tightened with respect to [4]: it is required that the output variable be greater than -13. The low Δm selection is used for $\Delta m < 12$ GeV/c^2 and the high Δm selection for $\Delta m \geq 12$ GeV/c^2. Sliding cuts, i.e. cuts depending on the mass hypothesis considered, are finally applied on the lepton momenta. Before those cuts, a total of 32.8 background events are expected in the search for acoplanar electrons and 29.6 in the search for smuons.

For the acoplanar tau analysis at high Δm, the visible mass is required to be less than 80 GeV/c^2 to reduce the four-fermion background. For both the high Δm and low Δm selections, correlations between the missing momentum and other kinematic variables such as $M_{\rm vis}$, the polar angle θ of the missing momentum and the ρ variable [13] are taken into account. A sliding cut on the energies of the τ's has been applied. The reconstructed τ is required to have an energy smaller than the maximum kinematically allowed for a given combination of mass hypotheses. Because of the higher luminosity, cuts on the momenta p_1, p_2 of the identified electrons and muons must be tightened with respect to [4]. The complete list of cuts of the stau analysis is summarised in Table 2. The low Δm selection is used for $\Delta m < 30$ GeV/c^2 while for $\Delta m \geq 30$ GeV/c^2 the high Δm selection is used. Before sliding cuts are applied, a total background of 15.5 events is expected for this selection.

3.4 Single electron selection

The search for single electrons is designed to select the signal expected from the mixed selectron production. The selection described in [4] has been optimized without changes in the selection strategy. The expected background from Weν and Zee processes is subtracted in

Table 2: Selection criteria for the searches for acoplanar taus (energy=[GeV], mass=[GeV/c^2], momentum=[GeV/c], angle=[degrees]).

	$\Delta m \geq 30$	$\Delta m < 30$
charged tracks	two identified τ's	
neutral veto	yes	
energy within 12° from beam	$E_{12} = 0$	
acollinearity	$\alpha > 2$	
visible mass	$M_{\rm vis} > 4$ $M_{\rm vis} < 80$	
acoplanarity	$\rho > (\Phi_{Aco} - 150)/8$	
missing momentum	$p_T^{miss} > 15 - M_{\rm vis}/4$ $p_T^{miss} < 1.14(\theta - 10)$	$M_{\rm vis} > 30$ or $p_T^{miss} > 5$ $\theta > 10$
ρ variable		$p_T^{miss} > 15 - 2\rho$
identified e and μ	$p_{T1}, p_{T2} > 0.5\%\sqrt{s}$ $p_1, p_2 < 23$	$p_1, p_2 < 13$
energy of τ	$E_\tau < E_{max}(m_{\tilde{\tau}}, m_\chi)$	

the optimization of the analysis. A total of 12.4 background events is expected, dominated by the Weν and Zee processes.

3.5 Results of the selections

A total of eight events are find in the data by the $\tilde{\rm t} \to {\rm c}\chi$ analysis: five by the high Δm selection (4.0 events expected) and three by the low Δm selection (5.5 events expected).

In the $\tilde{\rm b} \to {\rm b}\chi$ channel no events are selected in the data by the high Δm analysis (0.9 expected) and three events by the low Δm search (3.3 expected); these events are the same as those selected by the low Δm $\tilde{\rm t} \to {\rm c}\chi$ analysis.

In total, the acoplanar jet $\tilde{\rm t}$ and $\tilde{\rm b}$ analyses observe eight events, in good agreement with the expectation of 9.5 events from Standard Model processes.

The $\tilde{\rm t} \to {\rm b}\ell\tilde{\nu}$ analyses select two and zero events in the high and low Δm cases, respectively. The number of expected events are 0.4 and 1.9, respectively.

Before sliding cuts a total of 33 events are observed in the search for acoplanar electrons, 28 in the search for smuons and 21 in that for staus; the expected backgrounds are 32.8, 29.6, and 15.5 respectively. A total of eight events are observed in the single electron search, with 13.8 expected, mainly from four-fermion processes.

4 Systematic uncertainties

The systematic uncertainties on the selection efficiencies originating from the Monte Carlo simulation of the signal processes, as well as those related to detector effects, are evaluated following the procedure described in Refs. [3, 4]. The relative uncertainty on the selection efficiency in the case of $\tilde{\mathrm{t}} \to \mathrm{c}\chi$ is 13% for low Δm and 6% for high Δm; in the case of $\tilde{\mathrm{t}} \to \mathrm{b}\ell\tilde{\nu}$ it is 16% for low Δm and 7% for high Δm; for the $\tilde{\mathrm{b}} \to \mathrm{b}\chi$ channel it is 12% for low Δm and 6% for high Δm. These errors are dominated by the uncertainties on the simulation of $\tilde{\mathrm{t}}$ and $\tilde{\mathrm{b}}$ production and decay. The systematic uncertainties on the slepton selections amount to 3% for selectrons and smuons and up to 5% for staus.

The uncertainties on the evaluation of the subtracted backgrounds range from 3% to 9% depending on the selection and on the Δm considered.

The beam-related background is not included in the event simulation and is taken into account separately by using data collected at random beam crossings. The net effect is a relative decrease of the signal efficiency and the background expectation by 4%–8% depending on the studied selection. The systematic uncertainties on this correction are negligible.

5 Interpretation in the MSSM

The non-observation of any excess of candidates can be interpreted as lower limits on the masses of the particles searched for. The systematic uncertainties on the selection efficiencies are included following the method described in [14]. For slepton processes, the dominant sources of expected background (WW processes for the acoplanar lepton selections, Zee and Weν for the single electron) are subtracted according to the prescription of Ref. [15]. These subtracted backgrounds are reduced by their systematic uncertainties in the evaluation of the limits. No background subtraction is performed in interpreting the results of the searches for squarks. The limits are derived by combining the results presented here with the previous ALEPH ones [3, 4].

5.1 Squark mass lower limits

The regions excluded at 95% C.L. in the plane $(m_{\tilde{\mathrm{t}}}, m_\chi)$ are shown in Fig. 1a under the hypothesis of a dominant $\tilde{\mathrm{t}} \to \mathrm{c}\chi$ decay, and for two values of the $\tilde{\mathrm{t}}$ mixing angle $\theta_{\tilde{\mathrm{t}}}$, 0° and 56°, corresponding to maximal and minimal cross section, respectively. For Δm in the range from 10 to 40 GeV/c^2 the lower limit on $m_{\tilde{\mathrm{t}}}$ is 84 GeV/c^2, independent of $\theta_{\tilde{\mathrm{t}}}$.

Under the assumption of a dominant $\tilde{\mathrm{t}} \to \mathrm{b}\ell\tilde{\nu}$ decay and equal branching ratios for ℓ = e, μ and τ, the excluded region in the plane $(m_{\tilde{\mathrm{t}}}, m_{\tilde{\nu}})$ is shown in Fig. 1b. Assuming $\Delta m >$ 10 GeV/c^2 and using the LEP 1 lower limit on the sneutrino mass of 43 GeV/c^2 (calculated assuming three mass degenerate $\tilde{\nu}$'s), the $\theta_{\tilde{\mathrm{t}}}$ independent lower limit on $m_{\tilde{\mathrm{t}}}$ is, in this case, 86 GeV/c^2.

The excluded region in the plane $(m_{\tilde{\mathrm{b}}}, m_\chi)$ is shown in Fig. 2a under the assumption of a dominant $\tilde{\mathrm{b}} \to \mathrm{b}\chi$ decay. A lower limit of 86 GeV/c^2 is set on $m_{\tilde{\mathrm{b}}}$, assuming the $\tilde{\mathrm{b}}$ mixing angle $\theta_{\tilde{\mathrm{b}}} = 0°$ (corresponding to the case of maximal cross section) and $\Delta m > 10$ GeV/c^2. The

region excluded for $\theta_{\tilde{\mathrm{b}}} = 68°$, for which the cross section is minimal, is also shown in Fig. 2a; the comparison with the result from data collected in '97 up to $\sqrt{s} = 184$ GeV [3], also shown in the figure, clearly shows the substantial improvement in sensitivity thanks to the high statistics of the data sample collected at $\sqrt{s} = 188.6$ GeV.

As discussed in detail in Ref. [3], the negative results of the search for acoplanar jets, with or without b tagging, can also be interpreted as a lower limit on the mass of degenerate squarks. In order to compare the results directly with those obtained at the Tevatron, the limits have been evaluated under the following assumptions: a degenerate mass $m_{\tilde{\mathrm{q}}}$ for left-handed and right-handed $\tilde{\mathrm{u}}, \tilde{\mathrm{d}}, \tilde{\mathrm{c}}, \tilde{\mathrm{s}}, \tilde{\mathrm{b}}$; GUT relation between the soft supersymmetry breaking terms M_i associated with the $SU(2)_L \times U(1)_Y \times SU(3)_C$ gauge group, relating the gluino and neutralino masses; $\tan\beta = 4$ and $\mu = -400$ GeV. Under these assumptions, the ALEPH results can be translated into an exclusion region in the plane $(m_{\mathrm{gluino}}, m_{\tilde{q}})$, as shown in Fig. 2b.

In all these squark searches there is an improvement over the Tevatron exclusions [6, 7] in the region of small mass differences.

5.2 Slepton mass lower limits

The region excluded at 95% C.L. in the planes $(m_{\tilde{\mathrm{e}}}, m_\chi)$ and $(m_{\tilde{\mu}}, m_\chi)$ and the expected sensitivity are shown in Figures 3a and 3b assuming a dominant $\tilde{\ell}_R \to \ell\chi$ decay. For large $m_{\tilde{\ell}}$ and small neutralino masses, cascade decays such as $\tilde{\ell}_R \to \ell\chi'$ can play a role. Assuming $\tan\beta = 2$ and $\mu = -200\,\mathrm{GeV}/c^2$, as well as vanishing selection efficiency for final states deriving from cascade decays, reduces the excluded region as shown in the figures. For $\Delta m > 8$ GeV/c^2 selectron masses below 88 GeV/c^2 and for $\Delta m > 5$ GeV/c^2 smuon masses below 80 GeV/c^2 are excluded at 95% C.L.

In the case of staus, an additional degree of freedom affecting the production cross section comes from possible mixing between the left and right interaction eigenstates. The regions excluded at 95% C.L. in the plane $(m_{\tilde{\tau}}, m_\chi)$ assuming a dominant $\tilde{\tau}_1 \to \tau\chi$ decay are shown in Fig. 3c for the mixing cases corresponding to minimal cross section and pure right-handed $\tilde{\tau}$. The expected sensitivity in the latter case is also shown. For $\Delta m > 10$ GeV/c^2 stau masses below 66 GeV/c^2 are excluded at 95% C.L.; for $\Delta m > 13$ GeV/c^2 stau masses below 71 GeV/c^2 are excluded in the case of no mixing.

Assuming a common scalar mass at the GUT scale, the relation between the masses of the right- and left-handed sleptons can be used to combine results of the searches for acoplanar leptons and the search for events with single electrons. The region of the plane $(m_{\tilde{\ell}_R}, m_\chi)$ excluded at 95% C.L. for $\tan\beta = 2$ and $\mu = -200$ GeV and the expected sensitivity are shown in Fig. 3d. The loss of sensitivity of the $\tilde{\mathrm{e}}_{\mathrm{R}}\bar{\tilde{\mathrm{e}}}_{\mathrm{R}}$ search for very low values of Δm (< 3 GeV/c^2) is recovered for $m_{\tilde{\ell}} < 68$ GeV/c^2 by the search for $\tilde{\mathrm{e}}^{\pm}_{\mathrm{R}}\tilde{\mathrm{e}}^{\mp}_{\mathrm{L}}$. The effect of cascade decays at low m_χ is compensated by the search for $\tilde{\ell}_L\tilde{\ell}_L$ production.

6 Conclusions

In the data sample of 173.6 pb^{-1} collected in 1998 by the ALEPH detector at LEP at a centre-of-mass energy of 188.6 GeV, searches for signals from pair-production of the scalar partners of quarks and leptons have been performed. In all channels the number of candidates observed is consistent with the background expected from Standard Model processes.

In the MSSM the following lower mass limits are set at 95% C.L.:

- for stops:
  - 84 GeV/c^2, dominant $\tilde{\mathrm{t}} \to \mathrm{c}\chi$, $\Delta m > 10$ GeV/c^2;
  - 86 GeV/c^2, dominant $\tilde{\mathrm{t}} \to \mathrm{b}\ell\tilde{\nu}$, $\Delta m > 10$ GeV/c^2;
- for sbottoms:
  - 86 GeV/c^2, dominant $\tilde{\mathrm{b}} \to \mathrm{b}\chi$, $\Delta m > 10$ GeV/c^2, $\theta_{\tilde{\mathrm{b}}} = 0°$;
- for degenerate squarks:
  - 92 GeV/c^2, dominant $\tilde{q} \to \mathrm{q}\chi$, $\Delta m > 10$ GeV/c^2;
- for selectrons:
  - 88 GeV/c^2, $\Delta m > 8$ GeV/c^2, $\tan\beta = 2$ and $\mu = -200$ GeV/c^2;
  - 68 GeV/c^2, any Δm, $\tan\beta = 2$ and $\mu = -200$ GeV/c^2, common scalar mass at GUT scale;
- for smuons:
  - 80 GeV/c^2, dominant $\tilde{\mu} \to \mu\chi$, $\Delta m > 5$ GeV/c^2;
- for staus:
  - 66 GeV/c^2, dominant $\tilde{\tau} \to \tau\chi$, $\Delta m > 10$ GeV/c^2, worst case mixing;
  - 71 GeV/c^2, dominant $\tilde{\tau} \to \tau\chi$, $\Delta m > 13$ GeV/c^2, right-handed stau.

Acknowledgements

We wish to congratulate our colleagues from the accelerator divisions for the continued successful operation of LEP at high energies. We would also like to express our gratitude to the engineers and support people at our home institutes without whom this work would not have been possible. Those of us from non-member states wish to thank CERN for its hospitality and support.

References

[1] For a collection of reviews see *Supersymmetry and Supergravity,* Ed. M. Jacob, North-Holland and World Scientific, 1986.

[2] K. Hikasa and M. Kobayashi, Phys. Rev. **D 36** (1987) 724;
M. Drees and K. Hikasa, Phys. Lett. **B 252** (1990) 127.

[3] ALEPH Collaboration, *Scalar quark searches in e^+ e^- collisions at $\sqrt{s}$ = 181-184 GeV,* Phys. Lett. **B 434** (1998) 189.

[4] ALEPH Collaboration, *Search for sleptons in e^+e^- collisions at centre-of-mass energies up to 184 GeV,* Phys. Lett. **B 433** (1998) 176.

[5] D0 Collaboration, *Search for Light Top Squarks in $p\bar{p}$ Collisions at $\sqrt{s} = 1.8$ TeV,* Phys. Rev. Lett. **76** (1996) 2222.

[6] CDF Collaboration, *Search for scalar top and scalar bottom quarks in $p\bar{p}$ collisions at $\sqrt{s} = 1.8$ TeV*, submitted to Phys. Rev. Lett.

[7] D0 Collaboration, *Search for Squarks and Gluinos in $p\bar{p}$ Collisions at $\sqrt{s}$ = 1.8 TeV,* Phys. Rev. Lett. **75** (1995) 618; CDF Collaboration, *Search for gluinos and squarks at the Fermilab Tevatron collider,* Phys. Rev. **D 56** (1997) 1357.

[8] OPAL Collaboration, *Search for Scalar Top and Scalar Bottom Quarks at $\sqrt{s}$= 189 GeV at LEP,* CERN-EP/99-036; *Search for Acoplanar Lepton Pair Events in e^+e^- Annihilation at $\sqrt{s}$ = 161, 172 and 183 GeV,* CERN-EP/98-122.

[9] ALEPH Collaboration, *ALEPH: A detector for electron-positron annihilation at LEP,* Nucl. Instrum. and Methods **A 294** (1990) 121.

[10] ALEPH Collaboration, *Performance of the ALEPH detector at LEP,* Nucl. Instrum. and Methods **A 360** (1995) 481.

[11] ALEPH Collaboration, *A Precise Measurement of $\Gamma_{Z\to b\bar{b}}/\Gamma_{Z\to hadrons}$,* Phys. Lett. **B 313** (1993) 535.

[12] J.-F. Grivaz and F. Le Diberder, *Complementary analyses and acceptance optimization in new particle searches,* LAL **92-37** (1992); ALEPH Collaboration, *Mass limit for the Standard Model Higgs Boson with the full LEP 1 ALEPH data sample,* Phys. Lett. **B 384** (1996) 427.

[13] ALEPH Collaboration, *Searches for new particles in Z decays using the ALEPH detector,* Phys. Rep. **216** (1992) 253.

[14] R.D. Cousins and V.L. Highland, Nucl. Instrum. and Methods **A 320** (1992) 331.

[15] R. M. Barnett et al. (Particle Data Group), Phys. Rev. **D 54** (1996) 1.

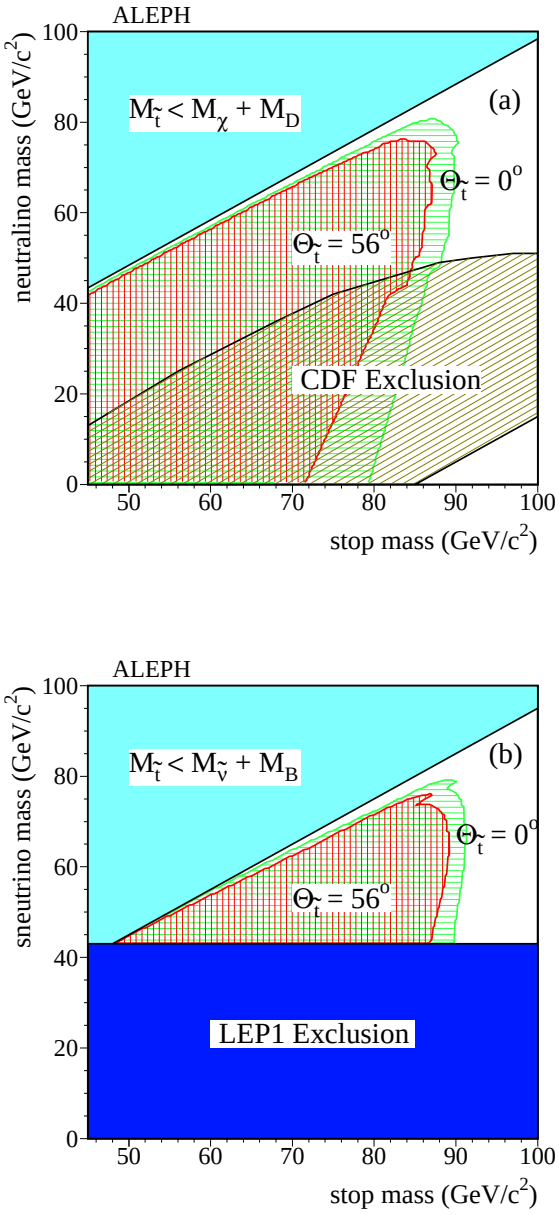

Figure 1: (a) Excluded regions at 95% C.L. in the m_χ vs $m_{\tilde{t}}$ plane from $\tilde{t} \to c\chi$ searches; the region excluded by the CDF experiment is also indicated. (b) Excluded regions at 95% C.L. in the $m_{\tilde{\nu}}$ vs $m_{\tilde{t}}$ plane from $\tilde{t} \to b\ell\tilde{\nu}$ (equal branching fractions for the $\tilde{t}$ decay to e, μ, and τ are assumed). The excluded regions are given for $\theta_{\tilde{t}} = 0°$, corresponding to maximum $\tilde{t}\tilde{t}Z$ coupling, and for $\theta_{\tilde{t}} = 56°$, corresponding to vanishing $\tilde{t}\tilde{t}Z$ coupling.

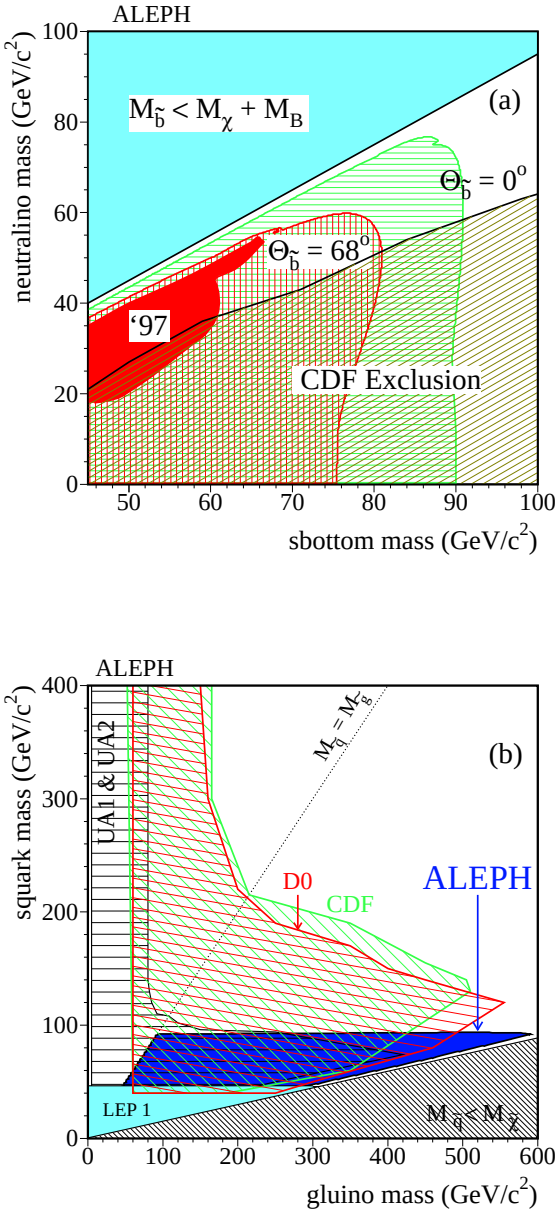

Figure 2: (a) Excluded regions at 95% C.L. in the m_χ vs $m_{\tilde{\mathrm{b}}}$ plane from $\tilde{\mathrm{b}} \to \mathrm{b}\chi$ searches; the region excluded by the CDF experiment is also indicated. The excluded regions are given for $\theta_{\tilde{\mathrm{b}}} = 0°$, corresponding to maximum $\tilde{\mathrm{b}}\tilde{\mathrm{b}}\mathrm{Z}$ coupling, and for $\theta_{\tilde{\mathrm{b}}} = 68°$ for which the '97 result is also shown, corresponding to vanishing $\tilde{\mathrm{b}}\tilde{\mathrm{b}}\mathrm{Z}$ coupling. (b) Excluded region from the search for generic $\tilde{\mathrm{q}}$ pairs, assuming five degenerate $\tilde{\mathrm{q}}$ flavours. The results are shown in the gluino-squark mass plane for $\tan\beta = 4$ and $\mu = -400\,\mathrm{GeV}/c^2$ together with results from experiments at $p\bar{p}$ colliders.

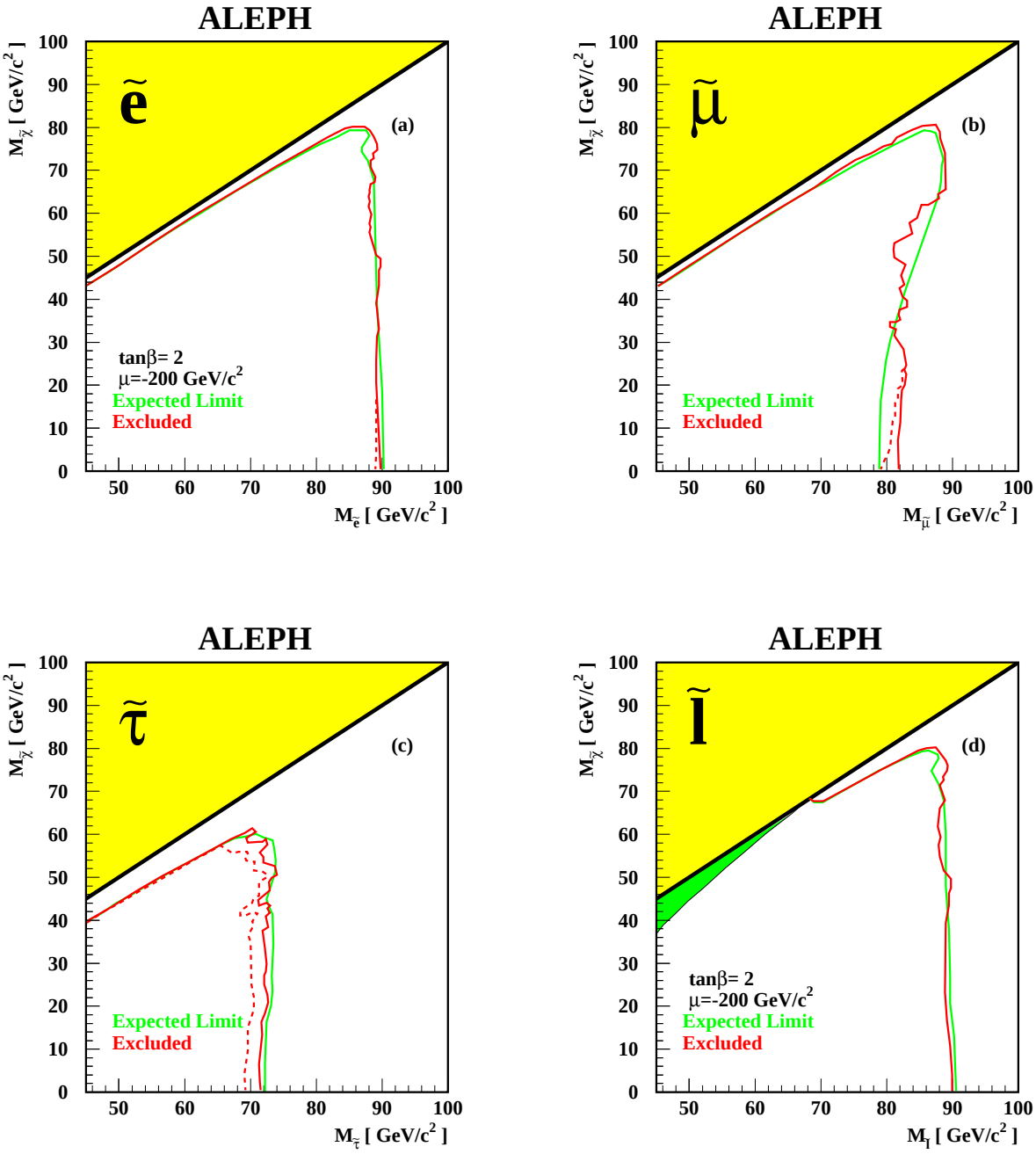

Figure 3: Excluded regions at 95% C.L. in the $m_{\tilde{\ell}_R}$ vs m_χ plane from slepton searches. BR($\tilde{\ell} \to \ell\chi$) = 100% is assumed for solid curves in (a) and (b) and all curves in (c). The dashed curves in (a) and (b) show the effect of cascade decays for $\tan\beta = 2$ and $\mu = -200\,\mathrm{GeV}/c^2$, assuming zero efficiency for those decays. The dashed curve in (c) shows the limit in the $m_{\tilde{\tau}_1}$ vs m_χ plane in the case of minimal $\tilde{\tau}_1\tilde{\tau}_1$Z coupling. In (d), the effect of cascade decays is included. The dark shaded region is not accessible because the common scalar mass at the GUT scale becomes unphysical.